N89-11139

# Migration Arising From Gradients in Shear Stress: Particle Distributions in Poiseuille Flow

D. T. Leighton, Jr.
University of Notre Dame
Notre Dame, IN 46556

Recent work has demonstrated that the time dependent properties exhibited by concentrated suspensions of non-colloidal spheres when sheared in a conventional Couette viscometer may be explained in terms of shear-induced particle migrations (Gadala-Maria and Acrivos, 1980; Leighton and Acrivos, 1987b). These suspensions were observed to exhibit both a short-term increase in viscosity upon shearing immediately after loading into the Couette device and a subsequent long-term decrease after prolonged shearing, which were used to estimate the effective shear-induced diffusivity for concentrated suspensions both normal to the plane of shear and parallel to gradients in fluid velocity within the plane of shear (Leighton and Acrivos, 1987b).

In this paper the experimental evidence for the existence of shear induced migration processes is reviewed and the mechanism proposed by Leighton and Acrivos (1987b) is described in detail. The proposed mechanism is shown to lead to the existence of an additional shear induced migration in the presence of gradients in shear stress such as would be found in Poiseuille flow, and which may be used to predict the amplitude of the observed short-term viscosity increase. The concentration and velocity profiles which result from such a migration are discussed in detail and are compared to the experimental observations of Karnis, Goldsmith and Mason (1966).

---

## 1. Introduction

Particle migrations across fluid streamlines in suspensions may result from a wide variety of mechanisms, ranging from Brownian type diffusive motions to the inertia induced drift mechanisms studied by Ho and Leal (1974) and others. In this paper we are concerned with *shear-induced* particle migrations which have been observed to occur in concentrated suspensions of non-colloidal particles (particles sufficiently large that colloidal forces are unimportant at distances comparable to the particle diameter) and at sufficiently low Reynolds numbers that inertial forces may be neglected. Particle migrations under these conditions have been observed by a number of researchers. Early work by Karnis and Mason (1967) demonstrated that particles tend to accumulate behind an advancing meniscus in flow through a tube, and to be depleted behind a receding meniscus, the magnitude of the phenomenon being a strong function of the particle diameter/tube radius ratio and the concentration, suggesting that the particle migration was the result of some type of wall effect. Leighton (1985) demonstrated that if proper precautions were not taken, this effect can lead to serious errors in viscosity measurements in concentrated suspensions. The coefficient of shear-induced self-diffusion of spheres in a sheared suspension (i.e., the diffusion or dispersion arising from a random walk of particles in a sheared suspension analogous to Brownian diffusion) was examined by Eckstein, Bailey and Shapiro (1977) and later by Leighton and Acrivos (1987a).

The observations of particle migration of primary interest here were initially made by Gadala-Maria and Acrivos (1980) in suspensions of 40μm to 50μm diameter polystyrene spheres in silicone fluids. In the course of viscometric measurements of concentrated suspensions made with a conventional Couette viscometer, Gadala-Maria and Acrivos (1980) found that the suspension viscosity would decrease after prolonged shearing, and eventually reach a steady-state value which was as much as a factor of two below the initially observed value (cf. Figure 1). In

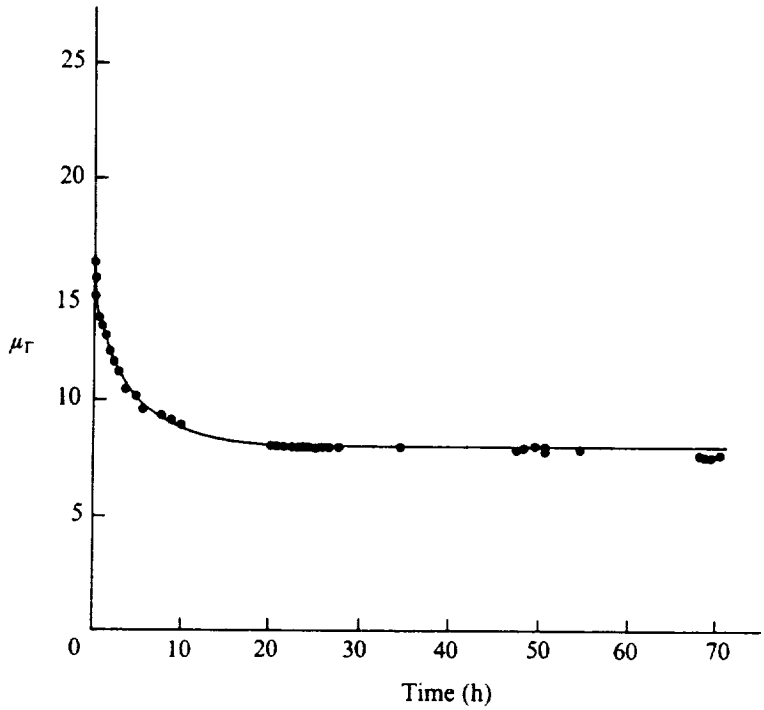


FIGURE 1 Relative viscosity of a $\phi = 0.45$ suspension as a function of the time that it had been sheared in the Couette device at $\dot{\gamma} = 24\ s^{-1}$. Polystyrene spheres, 40–50 μm in diameter in a mixture of silicone oils (from Gadala-Maria 1979, figure 33).

subsequent experiments, Leighton and Acrivos (1987b) demonstrated that the viscosity decrease was due to particle migration out of the sheared gap and into the reservoir by sealing the base of the Couette device with a layer of mercury and showing that the phenomenon disappeared. The rate of particle migration was found to be proportional to the shear rate and the square of the particle radius, and was successfully modelled by a one-dimensional diffusion process. The viscosity decrease was thus used to measure the effective diffusivity in the direction normal to the plane of shear for concentrated suspensions. The effective diffusivity was found to be a very strong function of concentration (cf. Figure 2) and to be much larger than the shear-induced coefficient of self-diffusion measured by Leighton and Acrivos (1987a).

During the course of their experiments (also with polystyrene spheres in silicone oils) Leighton and Acrivos (1987b) observed that, upon first shearing the suspension in the Couette device, the viscosity would increase over a total strain of approximately 100, reaching a steady-state value before the subsequent long-term viscosity decrease. Since the long-term viscosity decrease only became significant after a strain of about $10^3$ had elapsed, the two phenomena were well separated in time and could be investigated independently. As it is central to the present investigation into concentration distributions in Poiseuille flow, the short term viscosity decrease phenomenon is examined in more detail in the next section, which follows the development by Leighton and Acrivos (1987b).

## 2. Short-Term Viscosity Increase

The observed timescale appropriate to the initial viscosity increase phenomenon was found to be inversely proportional both to the shear rate $\dot{\gamma}$ and to the square of the ratio of the particle

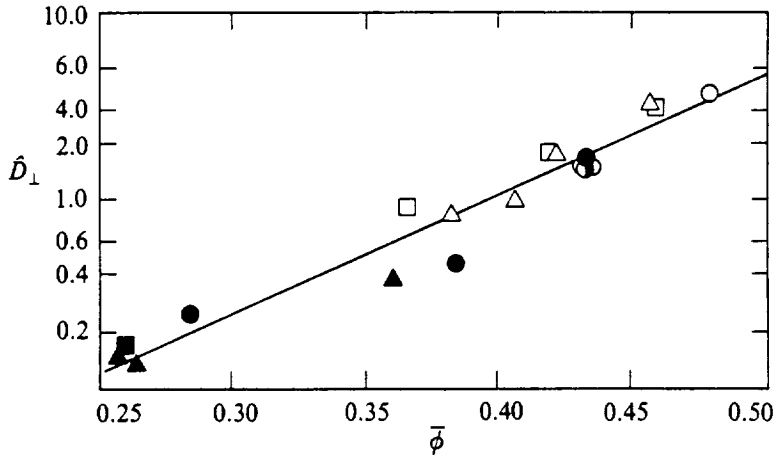


FIGURE 2 Diffusion coefficients calculated from the long-term viscosity decrease experiments: □, 46 μm polystyrene in 0.639 mm gap; ○, 46 μm polystyrene in 1.261 mm gap; △, 87 μm polystyrene in 1.261 mm gap. Shear rates were: filled symbols, 76 $s^{-1}$; open symbols, 24 $s^{-1}$; half-filled symbols, 7.6 $s^{-1}$.

diameter to gap width ratio $\hat{a}$; thus this effect was explained in terms of a shear-induced migration of particles across the width of the Couette gap analogous to the long-term viscosity decrease phenomenon. This could only be the case, however, if the suspension flowing into the gap during the loading procedure acquired a concentration distribution across the gap that was different from the equilibrium profile corresponding to Couette flow. Then, upon shearing, the particle distribution would diffuse into that appropriate for the Couette flow, and thereby induce a change in the observed viscosity. The actual change in the viscosity results from the non-linear dependence of the observed viscosity on the concentration profile. For example, if the concentration profile is only slightly non-uniform and is assumed to be symmetric about the centerline of the gap, then the observed viscosity may be calculated to be:

$$\frac{\mu_{obs}}{\bar{\mu}} - 1 = \frac{1}{\bar{\mu}}\left[\frac{1}{b}\int_0^b \frac{1}{\mu}dy\right]^{-1} = -\left[\left(\frac{1}{\mu}\frac{d\mu}{d\phi}\right)^2 - \frac{1}{2}\frac{1}{\mu}\frac{d^2\mu}{d\mu^2}\right]\Big|_{\bar{\phi}}\frac{1}{b}\int_0^b (\Delta\phi)^2 dy + O(\langle(\Delta\phi)^3\rangle) \qquad (2.1)$$

where the viscosity has been expanded in a Taylor series about $\phi = \bar{\phi}$. In equation 2.1, $\mu$ is the viscosity that corresponds to a uniform concentration $\bar{\phi}$, $\Delta\phi = \phi(y) - \bar{\phi}$ is the deviation from the average concentration across the gap, y = 0 denotes the centerline of the gap, and y = ±b the walls. Note that the variation in viscosity is proportional to the average value of $(\Delta\phi)^2$ across the gap for small fluctuations in concentration. The viscosity function in equation 2.1 may be calculated from the dependence of viscosity on concentration observed by Leighton and Acrivos (1987b):

$$\frac{\mu}{\mu_0} = \left[1 + \frac{\frac{1}{2}[\mu]\,\phi}{1 - \phi/\phi_m}\right]^2 \qquad (2.2)$$

an Eiler's equation where $\phi_m$ is the maximem particle concentration and $[\mu]$ is the intrinsic viscosity. The best fit values for the suspensions used in the experiments discussed here in the

range $.3 < \phi < .5$ were $\phi_m = 0.58$ and $[\mu] = 3.0$. From (2.2) it is found that any non-uniformity in concentration leads to a decrease in the observed viscosity, the magnitude of which is a strong function of the average concentration. Since the viscosity was observed to increase upon shearing, it was concluded that the initial concentration profile established upon loading the suspension into the gap was more non-uniform than that corresponding to Couette flow.

2.1. *Diffusion model for the observed short-term viscosity increase*

The viscosity increase phenomenon was modelled by assuming that the diffusion coefficient across the gap was constant throughout the migration. This approximation is acceptable if the variation in concentration is sufficiently small, and in any case the experiment yielded some average value of the diffusion coefficient for the migration. If the initial concentration profile is given by $\phi(0,y)$ and the concentration after a long period of shear is $\bar{\phi}$ (assumed to be constant), the concentration profile at all times is given by:

$$\phi(y,t) = \bar{\phi} + \sum_{n=1}^{\infty} B_n \cos\frac{n\pi y}{b} \exp\left(\frac{-n^2\pi^2 D_{\parallel} t}{b^2}\right) \qquad (2.3)$$

where

$$B_n = \frac{2}{b}\int_0^b \phi(0,y) \cos\frac{n\pi y}{b}\, dy$$

and $D_{\parallel}$ is the diffusivity within the plane of shear parallel to gradients in fluid velocity.

To further simplify the model, equation 2.3 was approximated by its limiting form at long times, i.e. the coefficients were chosen such that:

$$B_1 \neq 0; \quad B_n = 0, \quad n \neq 1 \qquad (2.4)$$

in which case, to obtain accurate values of the diffusion coefficient under this assumption, equation 2.3 was fitted only to data taken after sufficient time has elapsed for the neglected terms to become unimportant. Since these higher-order terms decrease exponentially with a rate constant at least four times that of the leading-order term, this requirement was easily met. Thus the model describing the short-term viscosity increase contains three adjustable parameters: the equilibrium uniform concentration; the amplitude of the initial variation in concentration $B_1$; and the diffusion coefficient. The first of these was fixed by the equilibrium viscosity corresponding to the concentration of the suspension initially loaded; thus the rate at which the viscosity approached its equilibrium value and the magnitude of the deviation between this and its value at the start of the experiment yielded the diffusion coefficient and the approximate initial concentration variation across the gap

It is important to note that the above development tacitly assumes that the concentration profile is not a function of the distance up the gap. In practice this is unlikely to be true since at the base of the gap the concentration profile will correspond to the entrance region into the gap, while sufficiently far up the gap it should correspond to the steady-state distribution resulting from Poiseuille flow. While this will be discussed in more detail in section 4, it is noted here that while variations in the initial concentration profile up the gap may affect the estimated amplitude of the concentration variation $B_1$, it should not affect the calculated value of $D_{\parallel}$. This arises from the assumption that the diffusivity is essentially constant within the gap, corresponding to the average concentration which does not vary along the length of the gap, and thus the rate at which the concentration approaches its steady-state distribution is the same at all positions along the gap.

2.2 *Experimental results*

Short-term viscosity increase experiments were performed by Leighton and Acrivos (1987b) with suspensions of 46μm and 87μm polystyrene spheres at concentrations from 30% to 50% in

two mixture of silicone oils with viscosities of 1.22p and 1.07p. The measurements were taken using Couette gap widths of 0.639mm, 1.261mm and 2.513mm. The gap height for all experiments was 4.508cm, and the bob diameter was 4.7498cm.

The fit of the data to the model was excellent (cf. Figure 3); however, owing to the many

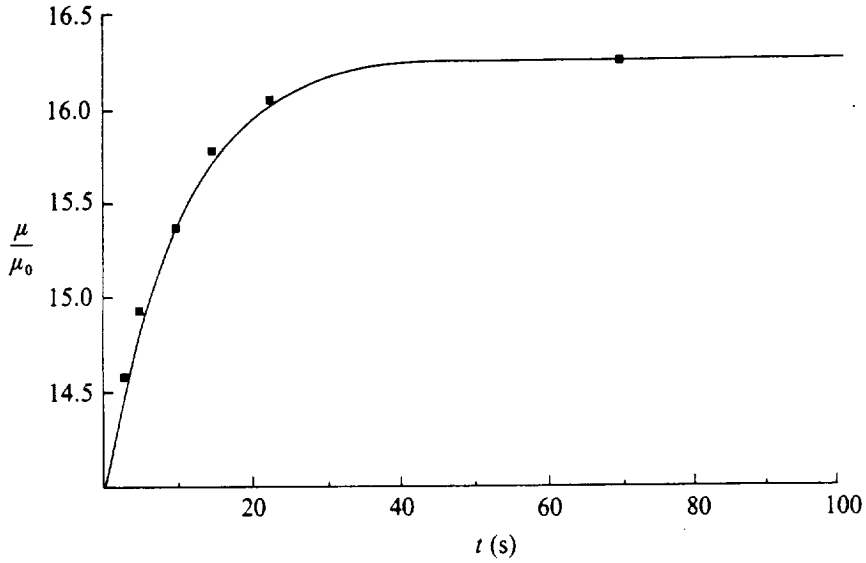


FIGURE 3 Short-term viscosity increase with shearing, 46 μm polystyrene suspension. Model parameters were: $\bar{\phi} = 0.45$, $\dot{\gamma} = 2.4\ s^{-1}$, $\hat{D}_{\|} = 1.8$, $B_1 = 0.062$.

assumptions that were necessary in deriving (2.3), the calculated values of the diffusion coefficient and concentration fluctuation across the gap must be considered only approximate. The diffusion coefficient was found to be proportional to $\dot{\gamma}a^2$ and, as in the case of diffusion normal to the plane of shear measured in the long-term viscosity decrease experiments, was a strong function of concentration. A plot of the diffusion coefficient as a function of concentration is given in Figure 4, where the dashed line is the diffusion coefficient normal to the plane of

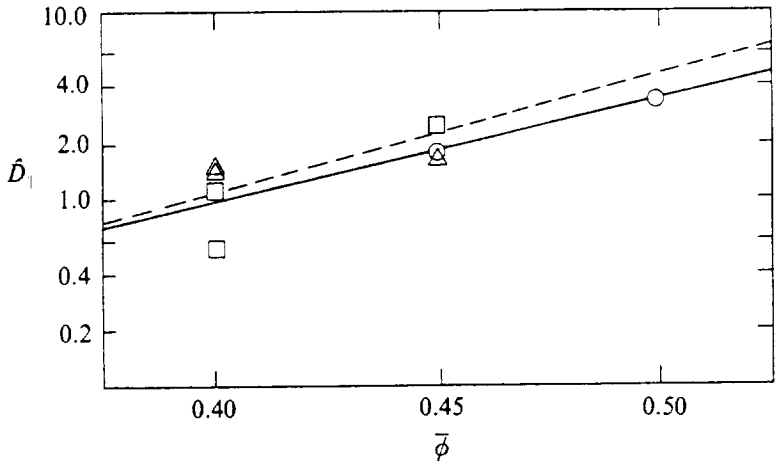


FIGURE 4 Diffusion coefficient observed in the short-term viscosity-increase experiments: ○, 46 μm polystyrene in medium gap; □, 46 μm polystyrene in small gap; △, 87 μm polystyrene in medium gap. Dashed line is the diffusion coefficient observed in the long-term viscosity-decrease experiments.

shear. The fact that the measured values of the two diffusion coefficients were almost identical provides us with added confidence that the viscosity increase was interpreted correctly as resulting from a particle migration across the gap width.

The short-term viscosity increase phenomenon was observable only for a narrow range of particle diameters, suspension concentrations and Couette gap widths. This was due in part to the fact that, since the diffusion coefficient was found to be proportional to the square of the particle radius, the total length of shearing necessary to reach steady-state was inversely proportional to $\hat{a}^2$, the square of the ration of the particle diameter to gap width. Thus, for very large values of $\hat{a}$ (such as were obtained for experiments with the 87μm polystyrene spheres in the narrow Couette gap) the strain associated with the migration was sufficiently short that it was not possible to reliably separate fluctuations in the viscosity due to migrations across the gap from those due to the initial equilibration of any short range order in the suspension, first observed by Gadala-Maria and Acrivos (1980). Similarly, the timescale for the viscosity increase was also much too short for experiments with the 46μm spheres in the narrow gap and a 50% concentration, owing to the high value of the dimensionless diffusion coefficient found at this concentration.

At 30% solids concentration, a different experimental difficulty was encountered in that, although the total fluctuation in concentration across the gap may have been the same as that observed for more concentrated suspensions, the resultant variation in the observed viscosity was too small to be accurately measured. From the observed dependence of viscosity on concentration, the same fluctuation in concentration across the width of the gap affects the observed viscosity at an average concentration of 30% by an amount that is less by an order of magnitude than that at 50%.

Finally, for some combinations of concentration, particle diameter and gap width, the short-term viscosity increase effect was not observable. No useable measurements were obtained for tha suspensions of either 46μm or 87μm spheres in the large Couette gap at concentrations of 30% to 45%, and for suspensions of 46μm spheres at 30% to 40% concentration in the medium Couette gap. Possible causes for the absence of a measurable initial increase will be discussed in section 4. Table 1 presents the calculated amplitude of the concentration fluctuation across the channel for those experiments where it was measurable.

| Particle diameter (μm) | Gap width (mm) | $\phi$ | $\hat{D}_1$ | $B_1$ |
|---|---|---|---|---|
| 46 | 0.639 | 0.40 | 1.1 | 0.131 |
| | | 0.40 | 0.54 | 0.094 |
| | | 0.45 | 2.45 | 0.075 |
| | 1.261 | 0.45 | 1.7 | 0.062 |
| | | 0.50 | 3.2 | 0.081 |
| 87 | 1.261 | 0.40 | 1.4 | 0.050 |
| | | 0.40 | 1.4 | 0.075 |
| | | 0.45 | 1.6 | 0.063 |

TABLE 1. Estimated diffusion coefficient and amplitude of concentration fluctuation for the short-term viscosity-increase experiments

## 3. Mechanisms leading to shear-induced migration

Thus far, we have presented experimental evidence for the existence of shear-induced particle migrations arising from gradients in concentration and shear stress. To see how these migrations take place we follow the development provided by Leighton and Acrivos (1987b). Let us first examine the case of migration due to gradients in particle concentration.

Consider a single marked sphere of radius **a** in a suspension of otherwise identical spheres undergoing the viscous linear shear flow $u = \dot{\gamma}y$, where u is the velocity in the x-direction. As the sphere interacts with its neighbors in the shear flow, it will experience a series of displacements in both the y- and z-directions with a characteristic length proportional to **a** and a frequency proportional to the shear rate $\dot{\gamma}$. In the absence of any gradient in concentration, these displacements will be random with zero mean (i.e. on average the particle will remain on its initial streamline), and thus will constitute a random walk. But, as is well known, in the presence of a concentration gradient such a random walk will lead to a diffusive flux and thus may be characterized by a diffusion coefficient, in this case with the dimensional scaling $\dot{\gamma}a^2$, the same as was observed in the experiments described here. It is important to note that in a dilute suspension the spheres will return to their initial streamlines at the end of all two-particle interactions owing to the linearity of the viscous-flow equations when only viscous forces are present. As a consequence, at least three particles must interact to yield the permanent displacements that lead to a random walk, and therefore, since the reate at which two particles interact with the marked sphere is proportional to $\dot{\gamma}\phi^2$, the diffusion coefficient must be proportional to $\phi^2\dot{\gamma}a^2$ in the dilute limit.

This source of diffusive flux, termed shear-induced self-diffusion, may be measured by examining the random walk of a single marked particle in a homogeneous suspension. Experiments carried out along these lines have been conducted by Eckstein, Bailey & Shapiro (1977), and more recently by Leighton & Acrivos (1987a), and have demonstrated that the diffusion coefficient is indeed proportional to $\dot{\gamma}a^2$. Leighton & Acrivos (1987a) also obtained a dimensionless value of the diffusivity of about $\phi^2/2$ in the dilute limit, in agreement with the scaling predicted by the theory. The measured coefficient of self-diffusion, however, was found to be a much weaker function of concentration and, at a concentration of 40%, had a value nearly an order of magnitude lower than the diffusivity that was calculated from the experiments described earlier in this work. The discrepancy between the observations of self-diffusion and effective diffusivity in the presence of a gradient in concentration suggests, therefore, that the presence of a concentration gradient in some way induces a drift of particles from regions of high to low concentration in addition to that provided by random self-diffusion.

The most likely source of this additional drift is that interparticle interactions in the presence of a gradient in concentration lead to an average displacement of the marked sphere from regions of high to low concentration. It is not clear at this stage whether interactions in the presence solely of viscous forces can lead to such a drift. Direct calculations of the drift for such a suspension would require consideration of interactions involving at least three spheres in a dilute suspension and, in concentrated suspensions where the average interparticle separation distance is very small, the interaction of many spheres would have to be taken into account. Such calculations are far beyond the capabilities of current analytical techniques, and are also quite difficult to deal with numerically owing to the very large number of particles that must be included in any computation.

As we shall presently demonstrate, however, for sufficiently concentrated suspensions of real non-colloidal particles, it is not necessary or even appropriate to consider only the influence of purely viscous hydrodynamic forces because, in such systems, the particles are driven sufficiently close together by the flow that irreversible surface contact will occur as a consequence of surface-roughness effects, thereby destroying the macroscopic reversibility of the purely viscous interactions. In this section we shall therefore discuss both theoretical and experimental evidence for the existance of such irreversible interactions and demonstrate that they may lead to

the diffusivities observed here.

3.1. *Irreversible interactions in concentrated suspensions*

Consider a sphere interacting with a second sphere in a simple shear flow. As the two spheres approach one another, the viscous stresses in the fluid act to drive the spheres together. Under purely viscous conditions, when the interparticle separation distance is very small this approach is resisted by the lubrication layer between the particles, in which the resistance is inversely proportional to the separation distance. Thus although two mathematically smooth interacting spheres may never touch, hydrodynamic theory predicts that, over a certain range of initial configurations, they will approach one another very closely even in a dilute suspension. On the other hand, in the presence of a finite amount of surface roughness on the spheres (as is the case for any real particles), the interaction may be significantly modified. Indeed, Arp & Mason (1977) found that even for two isolated interacting spheres, the existence of a small degree of surface roughness was sufficient to eliminate the closed orbits predicted for purely viscous interactions.

This effect of surface roughness is accentuated for concentrated suspensions. Specifically, since the forces driving spheres together in the flow depend on the bulk fluid stresses, they are proportional to the bulk suspension viscosity, which in turn is a strong function of concentration. In contrast, the lubrication forces resisting this approach remain proportional to the pure-fluid viscosity since the presence of other particles in the suspension does not affect the flow in the narrow gap between particles. This imbalance, combined with some finite surface roughness, implies that in sufficiently concentrated suspensions particles will simply approach one another without any significant displacemtn from the their original streamlines until they come into physical contact, folowing which they will rotate owing to the vorticity of the shear flow, and finally separate. Moreover, since the interaction is no longer reversible owing to the surface contact it will also no longer be symmetric and thus will lead to permanent displacemtns of the particles from their original streamlines at the end of each interaction. A more complete discussion of the evidence for irreversible interactions and thier effect on the rheology of concentrated suspensions is given by Leighton (1985).

3.2 *Particle drift arising from irreversible interactions*

There are several ways in which the irreversible interactions described above can lead to drift in the presence of gradients in concentration or shear stress. To see this, consider a test sphere at the origin which is immersed in a suspension undergoing shear. We shall assume that the bulk flow is in the x-direction with a constant shear stress $\sigma = \sigma_{yx}$ and a linear concentration gradient in the z-direction, normal to the plane of shear. Under these conditions, the viscosity, and hence the shear rate, will be be constant within the plane of shear. Consequently, when the particles are not mathematically smooth, the test sphere will be irreversibly displaced upwards following an interaction with another sphere approaching it from below, and conversely if approached from above. Thus, in the presence of a higher particle concentraiton on one side of the test sphere than on the other, this sphere will experience a drift towards the region of lower concentration since it interacts with more particles on one side than on the other. Moreover, the displacement after each interaction will be proportional to the particle radius; thus since the excess rate of interactions from regions of higher concentration is proportional to $\dot{\gamma}ad\phi/dz$, the particle flux resulting from this source of drift should be proportional to $\dot{\gamma}a^2\phi d\phi/dz$, which is the same scaling expected for shear-induced diffusion.

A second source of drift normal to the plane of shear arises from the gradients in suspension viscosity brought about by gradients in concentration. First we note that in the absence of a gradient in viscosity, two touching spheres in a shear field will rotate about their center of mass (the point of contact). But, in the presence of a viscosity gradient, the center of mass will no longer be the center of rotation and the particles will, on average, be displaced during an interaction from regions of high to low viscosity. The magnitude of this displacement during each irreversible interaction will scale as the relative variation in viscosity across the

particle, i.e. it will be proportional to $(a/\mu)d\mu/dz$, multiplied by the particle radius. Since, for small gradients in concentration, the variation in viscosity is linear in the concentration gradient, the above result, when multiplied by the rate of interactions $\dot{\gamma}\phi$, gives the corresponding drift velocity. In turn, when multiplied by $\phi$ and divided by $d\phi/dz$, the drift velocity leads to an expression for the effective diffusivity arising from this source of drift $D \sim \dot{\gamma}a^2(\phi^2/\mu)d\mu/d\phi$. The total effective diffusivity normal to the plane of shear is then the sum of the two mechanisms outlined above, plus that due to shear induced self-diffusion.

For concentrated suspensions, the function $(1/\mu)d\mu d\phi$ is very large, with a value of about 15 for a 45% suspension; thus drift due to gradients in viscosity is likely to dominate the diffusivity. Recognizing this, we therefore let

$$D_\perp = K_\perp \frac{\phi^2}{\mu}\frac{d\mu}{d\phi}\dot{\gamma}a^2 \qquad (3.1)$$

be the expected form for the effective diffusivity normal to the plane of shear at high concentrations, where $K_\perp$ is a dimensionless parameter whose value will depend on the exact geometry of the interactions. As shown in figure 5, $K_\perp$, as determined from the results of the long-term viscosity experiment, was found to be a relatively weak function of concentration with a value of about 0.7 at 45%. The scatter in the data is, of course, indicative of the simplcity of the model.

The contribution of irreversible interactions to drift within the plane of shear is quite similar to that found above for the case of drift normal to the plane of shear. Again, displacements will lead to random self-diffusion, to drift arising from a higher rate of interactions on one side than on another due to the concentration gradient (assuming a uniform shear rate), and drift from regioins

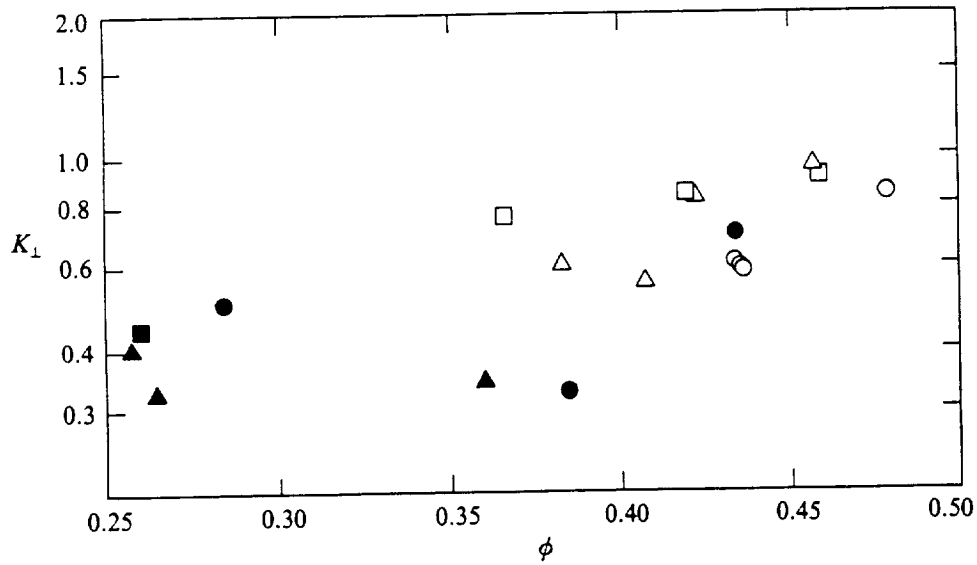


FIGURE 5 Value of $K_\perp$ *vs.* concentration: □, 46 μm polystyrene in 0.639 mm gap; ○, 46 μm polystyrene in 1.261 mm gap; △, 87 μm polystyrene in 1.261 mm gap. Open symbols, $\dot{\gamma} = 24\ s^{-1}$; filled symbols, $\dot{\gamma} = 76\ s^{-1}$; half-filled symbols, $\dot{\gamma} = 7.6\ s^{-1}$.

of high to low viscosity. In addition to these sources of drift, however, variations in viscosity within the plane of shear will, in the case of a uniform applied shear stress, lead to variations in the local shear rate. Thus, in regions of low concentration and low viscosity the shear rate will be greater, with the consequence that a test sphere will, on average, experience a greater number of interactions from the region of lower concentration than would otherwise be the case. Since the shear rate is inversely proportional to the local viscosity for a constant shear stress, the excess rate

of such interactions will be proportional to $(\phi\dot{\gamma}a/\mu)(d\mu/dy)$, which in turn will reduce the drift velocity from regions of high to low concentration by an amount proportional to $(\dot{\gamma}a^2\phi/\mu)(d\mu/d\phi)(d\phi/dy)$, an expression for the drift velocity identical with that due to gradients in viscosity with uniform shear.

Although this drift due to the shear rate gradient effect will certainly reduce the magnitude of the effective diffusivity (the sum of all contributions due to drift and random walk) it appears unlikely that the two terms due to gradients in fluid viscosity will exactly cancel out. Thus, as in the case of diffusion normal to the plane of shear, we obtain for the limiting expression of the effective diffusivity at high concentrations

$$D_{\parallel} = K_{\parallel}\frac{\phi^2}{\mu}\frac{d\mu}{d\phi}\dot{\gamma}a^2 \tag{3.2}$$

where the value of $K_{\parallel}$ may be determined from the initial-viscosity-increase experiments. The results are shown in Figure 6 from where it is seen that, in spite of the scatter, which again is indicative of the simplicity of the model, $K_{\parallel}$ appears to be relatively independent of concentration and approximately equal to 0.6.

The same mechanism due to gradients in shear rate that reduced the effective diffusivity within the plane of shear should also lead to drift from regions of high to low shear stress in a homogeneous suspension. This is because, for the case of uniform particle concentrations and uniform suspension viscosities, the local shear rate is proportional to the local shear stress $\sigma$; hence the excess rate of particles interacting with the test sphere from regions of high shear stress is proportional to $(\phi\dot{\gamma}a/\sigma)/(d\sigma/dy)$, yielding a particle flux

$$N_y = -K_{\sigma}\frac{\phi^2}{\sigma}\frac{d\sigma}{dy}\dot{\gamma}a^2 \tag{3.3}$$

where again $K_{\sigma}$ is some order-one function of concentration.

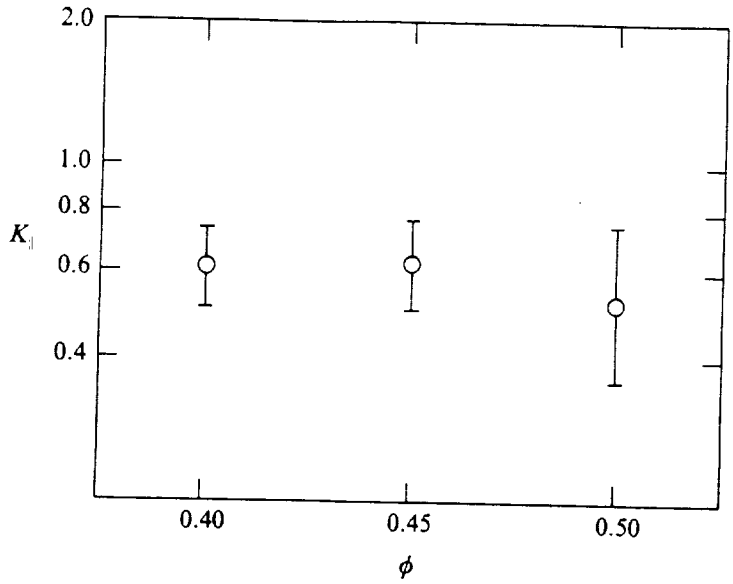


FIGURE 6 Average value of $K_{\parallel}$ *vs.* concentration calculated from the data in table 1. Error bars denote one standard deviation as estimated from the scatter in the experimental results.

## 4. Particle distributions in Poiseuille flow

Using the above analysis it is possible to determine the steady-state concentration distribution acquired by a concentrated suspension undergoing flow in a channel or a tube. Since the shear stress in Poiseuille flow is a maximum at the walls and zero in the center, migration due to the gradient in shear stress will result in a depleted concentration near the walls. At steady-state, this inward migration is balanced by shear-induced diffusive migration outwards, where the net particle flux:

$$N_y = -\left[K_\sigma \frac{\phi^2}{\sigma}\frac{d\sigma}{dy} + K_{\|}\frac{\phi^2}{\mu}\frac{d\mu}{d\phi}\frac{d\phi}{dy}\right]\dot{\gamma}a^2 \qquad (4.1)$$

is set equal to zero. For Poiseuille flow the shear stress is simply proportional to y, hence

$$\frac{1}{\sigma}\frac{d\sigma}{dy} = \frac{1}{y} \qquad (4.2)$$

and therefore we obtain the derivative of the steady-state concentration profile:

$$\frac{d\phi}{dy} = -\frac{K_\sigma}{K_{\|}}\left(\frac{1}{\mu}\frac{d\mu}{d\phi}\right)^{-1}\frac{1}{y} \qquad (4.3)$$

where the viscosity is a known function of concentration. If we assume that the ratio $K_\sigma/K_{\|}$ is approximately constant across the gap, then (4.3) may be directly integrated to yield the viscosity profile:

$$\frac{\mu}{\mu_w} = \left(\frac{b}{y}\right)^{\frac{K_\sigma}{K_{\|}}} \qquad (4.4)$$

where $\mu_w$ is the relative viscosity of the suspension evaluated at the concentration at the walls. Using the observed relationship between viscosity and concentration (given by equation 2.2), we may invert equation 4.4 to obtain the concentration profile across the channel:

$$\phi = \phi_m\left(1 + \frac{\frac{1}{2}[\mu]\phi_m}{\left[\mu_w\left(\frac{b}{y}\right)^{\frac{K_\sigma}{K_{\|}}}\right]^{1/2} - 1}\right)^{-1} \qquad (4.5)$$

which is a function only of the ratio $K_\sigma/K_{\|}$ and the concentration at the wall. Note that the concentration distribution given by equation 4.5 applies to both flow through channels and tubes. For a known value of $K_\sigma/K_{\|}$ the wall concentration may be determined from the average concentration by integrating 4.5 across the channel or, in the case of flow through a tube, by integrating the product $\phi 2rdr$. A plot of the expected concentration profile for $\phi$ as a function of $K_\sigma/K_{\|}$ is given in Figure 7 for $\phi = 0.45$. Note that the predicted concentration approaches the maximum value $\phi = \phi_m$ at y=0. This is a consequence of the singularity in (4.2), and the divergence of the effective diffusivity as the particle concentration approaches its maximum value.

### 4.1 *Estimation of* $K_\sigma$

We may estimate the value of $K_\sigma$ from the amplitude of the short-term viscosity increase phenomenon if we examine in more detail the procedure by which suspensions are loaded into the Couette device. As is described in detail by Leighton and Acrivos (1987b), in these experiments the fluid was loaded into the gap by first pouring the suspension into the Couette cup and then lowering the bob, thus displacing the fluid and filling the gap. The flow thus created consists of a converging entrance flow at the base of the gap, followed by channel flow up the gap. While it is unclear what effect, if any, the entrance flow has on the concentration profile, the channel flow up the gap should lead to a migration of the particles from the regions near the walls into the center. The concentration profile in the gap will thus be a function of distance up the gap, but provided that the height of the gap is sufficiently large the concentration profile in the gap will approach the steady-state distribution given by (4.5).

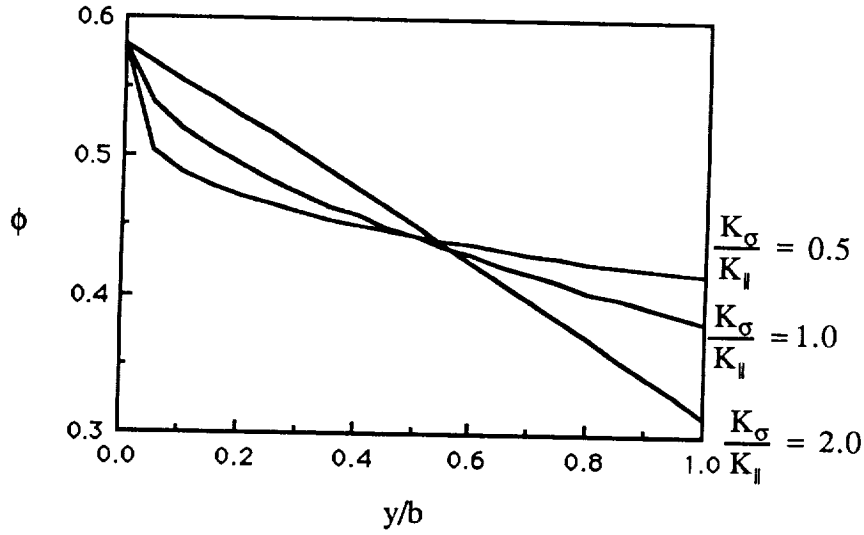


Figure 7. Plot of concentration profile across a channel predicted from equation 4.5 for an average concentration of 45%, as a function of $K_\sigma / K_\parallel$.

If we assume that the concentration profile in the gap is indeed due to migrations arising from gradients in shear stress we may estimate the influence of finite gap length on the short-term viscosity increase phenomenon. The concentration distribution in the gap will be governed by the differential equation:

$$u\frac{\partial \phi}{\partial x} = -\frac{\partial N_y}{\partial y} = \frac{\partial}{\partial y}\left\{ \hat{D}_\parallel \dot{\gamma} a^2 \left[\frac{\partial \phi}{\partial y} + \frac{K_\sigma}{\hat{D}_I}\frac{1}{y}\right] \right\} \qquad (4.6)$$

where:

$$u = u_m\left(1 - \frac{y^2}{b^2}\right) \; ; \; N_y\big|_{y=\pm b} = 0 \; ; \; \phi\big|_{x=0} = \phi_0$$

where, for purposes of estimation, we linearize the problem by assuming the velocity profile to be parabolic and the diffusivity to be constant, and where we have assumed a no-flux boundary condition at the sides of the channel and a uniform concentration at the entrance. The differential equation may be rendered dimensionless using the variables

$$y^* = \frac{y}{b} \; ; \; x^* = \frac{2\,x\,a^2\hat{D}_I}{b^3} \qquad (4.7)$$

resulting in the dimensionless equation:

$$(1 - y^{*2})\frac{\partial \phi}{\partial x^*} = \frac{\partial}{\partial y^*}\left\{ |y^*| \left[\frac{\partial \phi}{\partial y^*} + \frac{K_\sigma}{\hat{D}_I}\frac{1}{y^*}\right] \right\} \qquad (4.8)$$

where:

$$\frac{\partial \phi}{\partial y^*}\Big|_{y^* = \pm 1} = \pm\left(-\frac{K_\sigma}{\hat{D}_I}\right) \quad \text{and} \quad \phi\big|_{x^*=0} = \phi_0$$

which may be solved using separation of variables. Equation 4.8 admits a solution of the form:

$$\phi(x^*,y^*) = \phi_\infty(y^*) + \sum_{n=0}^{\infty} A_n \exp(-\alpha_n^2 x^*) F_n(y^*) \qquad (4.9)$$

with

$$A_n = \frac{\int_0^1 (1 - y^2) F_n(y)\left(\phi_\infty(y) - \phi_0\right) dy}{\int_0^1 (1 - y^2) F_n^2(y)\, dy}$$

where the eigenfunctions $F_n$ satisfy the Sturm-Liouville type equation:

$$\left(y^* F_n'\right)' + \alpha_n^2 (1 - y^{*2}) F_n = 0 \qquad (4.10)$$

with

$$F_n(0) = \text{finite} \; ; \; F_n'(1) = 0$$

While equation 4.10 does not admit a closed form solution, the leading eigenvalue has been determined numerically to be $\alpha_0 = 2.277795$. As a consequence, the assumption that the concentration distribution in the gap is close to that at steady-state for channel flow will be valid provided

$$\frac{2\,\alpha_0^2\, a^2 \hat{D}_{\parallel} h}{b^3} >> 1 \qquad (4.11)$$

where h is the gap height. In the experiments described by Leighton and Acrivos (1987b) where the short-term viscosity increase was observable, the dimensionless parameter given in (4.11) ranged from 1.9 to 14, thus the assumption of steady-state is reasonably good. In contrast, in those experiments where the short-term viscosity increase was not observed, the value of the parameter was less than 1, suggesting that the observed increase was, in fact, due to particle migrations in Poiseuille flow rather than entrance effects.

To estimate the value of $K_\sigma$, we may simply substitute the steady-state concentration distribution given by equation 4.5 into the equation for $B_1$ given in equation 2.3 and integrate. The resulting values of $K_\sigma$ are given in Figure 8, which, allowing for considerable scatter in the experimental data, indicates that $K_\sigma$ is a relatively weak function of concentration (not quite constant as we have assumed) with a value of about 0.6 at $\phi = 0.45$.

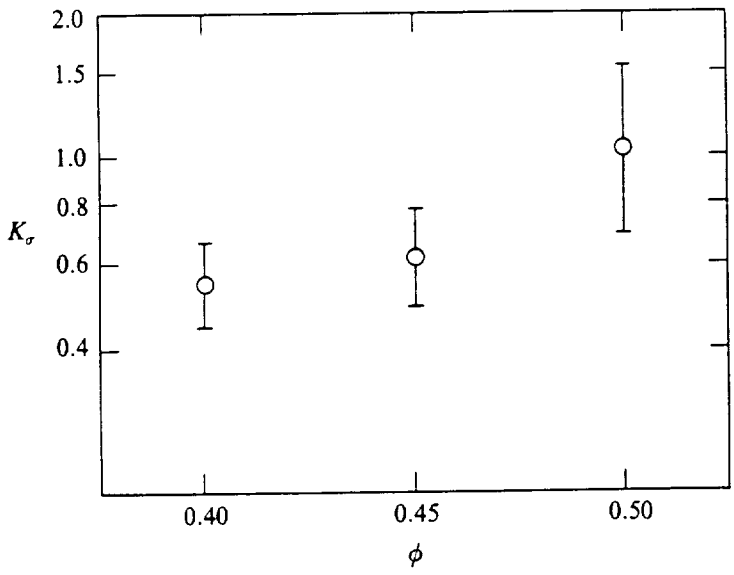


FIGURE 8 Average value of $K_\sigma$ *vs.* concentration calculated from the data in table 1. Error bars are one-standard-deviation error estimated from the scatter in the experimental results.

4.2 *Comparison with other experiments*

In a bounded Poiseuille flow (channel or tube), any migration of particles toward the center leads to an increase in the viscosity in this region and hence to a blunting of the parabolic velocity profile that applies for Newtonian fluids. We may calculate the expected velocity profile resulting from the steady-state viscosity distribution given in equation 4.4:

$$\frac{u}{u_m} = 1 - \left(\frac{y}{b}\right)^{2+K_\sigma/K_I} \qquad (4.12)$$

which, surprisingly, is not a function of concentration. Of course, in the development leading up to (4.4) we assumed that the ratio $K_\sigma/K_{II}$ is independent of concentration. This is certainly not true for dilute suspensions where the mechanisms leading to the shear stress gradient induced migrations would be expected to vanish, and is only approximately correct for concentrated suspensions.

Observations of velocity profiles in concentrated suspensions flowing through tubes were conducted by Karnis, Goldsmith and Mason (1966). Their observations at an average concentration of 38% (the highest concentration for which measurements were reported) and particle/tube diameter ratio of .028 is reproduced in Figure 9 together with the profile predicted by

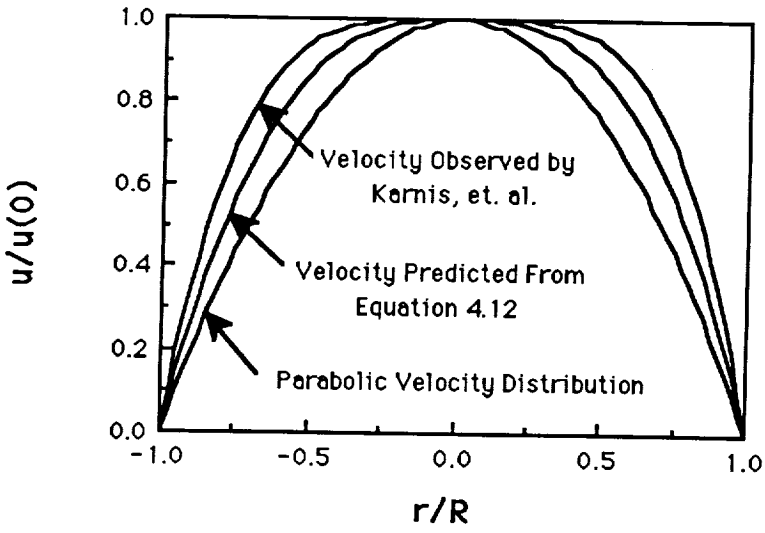


Figure 9. Comparison of the velocity distribution estimated from equation 4.12 with that observed by Karnis, et al. (1966).

equation 4.12 using an observed ratio $K_\sigma/K_{II} = .912$ estimated from the $\phi = 0.40$ experiments described above. From this comparison it is seen that the velocity profile observed by Karnis, *et al.* is blunter than that predicted here, corresponding to $K_\sigma/K_{II} \approx 2.1$. While these two values do not greatly differ considering the large degree of scatter in our experiments, at least part of the discrepancy may be accounted for by wall effects. Indeed, Karnis, Goldsmith, and Mason attributed their observed blunting entirely to wall effects, however in view of the small particle diameter / tube diameter used in the experiment depicted here, this seems unlikely. Experiments in the Couette geometry reported by Karnis, *et al.* (1966), showed that wall effects were insignificant at the same concentrations even for particle diameter / gap width ratios over a factor of three larger than that used in the experiments leading to Figure 9.

These authors did attempt to measure the concentration profile across a tube, although only at a lower average concentration of 32%. Owing to the statistical nature of their measurement technique, however, their observations had a very large experimental error. Specifically, their measurements involved counting the number of spheres that were present in each of four divisions of the half-width of a tube cross-section, and since only a small fraction of the spheres were marked, their observations were subject to Poisson statistics, which dictate that the one-standard-deviation error in the number of spheres that were counted is equal to the square root of that number. But since the total number of spheres that were counted in each region was rather small (less than 80), the concentrations reported by Karnis *et al.* (1966) had a two standard deviation error of nearly 25%. Their observations, with error estimated as described above, together with the concentration profile predicted using equation 4.5 and a value of $K_\sigma/K_{||} = .912$ is given in Figure 10. While the concentration observations of Karnis *et al.* do not agree with the predicted concentration profile (which has been extrapolated well beyond the range over which $K_\sigma/K_{||}$ was estimated), more accurate measurements of the concentration distribution in Poiseuille flow are needed in order to determine the source of the observed blunting of the velocity profiles.

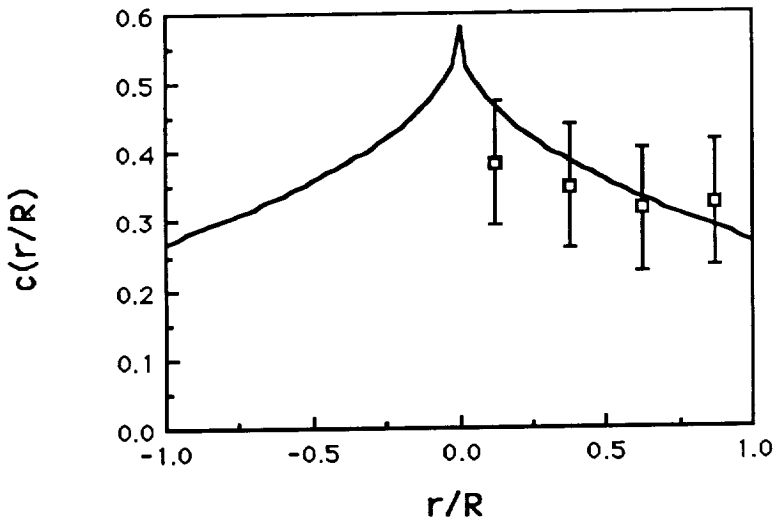


Figure 10. Comparison of concentration distribution estimated from equation 4.5 with particle distribution observed by Karnis, et al. (1966). Error given is 2 standard deviation error calculated by statistical means.

**Acknowledgements**

Portions of this paper were condensed from the referenced paper Leighton and Acrivos (1987b). This work was supported in part by the National Science Foundation.

---

**References:**

Arp, P. A. & Mason, S.G. 1977 The kinetics of flowing dispersions. IX. Doublets of rigid spheres (experimental). *J. Colloid Interface Sci.* **61**, 44.

Eckstein, E. C., Bailey, D. G. & Shapiro, A. H. 1977 Self-diffusion of particles in shear flow of a suspension. *J. Fluid Mech.* **79**, 191.

Gadala-Maria, F. 1979 The rheology of concentrated suspensions. Ph.D. thesis, Stanford University.

Gadala-Maria, F. & Acrivos, A. 1980 Shear-induced structure in a concentrated suspension of solid spheres. *J. Rheology* **24**, 799.

Ho, B. &Leal, L. 1974 Inertial migration of rigid spheres in two-dimensional uni-directional flows. *J. Fluid Mech.* **65**, 365.

Karnis, A., Goldsmith, H. L. & Mason, S. G. 1966 The kinetics of flowing dispersions. I. Concentrated suspensions of rigid particles. *J. Colloid Interface Sci.* **22**, 531.

Karnis, A. & Mason, S. G. 1967 The flow of suspensions through tubes. I. Meniscus effects. *J. Colloid Interface Sci.* **23**, 120.

Leighton, D. 1985 The shear induced migration of particulates in concentrated suspensions. Ph.D. thesis, Stanford University.

Leighton, D. & Acrivos, A. 1987 Measurement of self-diffusion in concentrated suspensions of spheres. *J. Fluid Mech.* **177**, 109.

Leighton, D. & Acrivos, A. 1987 Shear-induced migration of particles in concentrated suspensions. *J. Fluid Mech.* **181**, 415.